MNRAS **000**, 1–16 (0000) Preprint 9 December 2016 Compiled using MNRAS LATEX style file v3.0

X-ray flux variability of active galactic nuclei observed using NuSTAR

Priyanka Rani,* C. S. Stalin and Suvendu Rakshit
Indian Institute of Astrophysics, Koramangala, Bangalore 560034, India

Accepted 2016 December 08. Received 2016 December 08; in original form 2016 September 26

ABSTRACT

We present results on a systematic study of flux variability on hourly time scales in a large sample of active galactic nuclei (AGN) in the 3−79 keV band using data from NuSTAR. Our sample consists of 4 BL Lac objects (BL Lacs), 3 flat spectrum radio quasars (FSRQs) 24 Seyfert 1, 42 Seyfert 2 and 8 narrow line Seyfert 1 (NLSy1) galaxies. We find that in the 3−79 keV band, about 65% of the sources in our sample show significant variations on hourly time scales. Using Mann-Whitney U-test and Kolmogorov-Smirnov test, we find no difference in the variability behaviour between Seyfert 1 and 2 galaxies. The blazar sources (FSRQs and BL Lacs) in our sample, are more variable than Seyfert galaxies that include Seyfert 1 and Seyfert 2 in the soft (3−10 keV), hard (10−79 keV) and total (3−79 keV) bands. NLSy1 galaxies show the highest duty cycle of variability (87%), followed by BL Lacs (82%), Seyfert galaxies (56%) and FSRQs (23%). We obtained flux doubling/halving time in the hard X-ray band less than 10 min in 13 sources. For PKS 2155−304, we find the shortest flux doubling time of 1.65 ± 0.16 min the shortest known in the hard X-ray band from any blazar. The flux variations between the hard and soft bands in all the sources in our sample are consistent with zero lag.

Key words: galaxies: active−X-rays: galaxies.

1 INTRODUCTION

There is convincing evidence that accretion onto supermassive black holes powers active galactic nuclei (AGN; Rees 1984). A vast majority of about 85% of them emit little or no radio emission, these AGN are termed radio-quiet AGN and a minority of about 15% called radio-loud AGN have large scale relativistic jets and emit copiously in the radio band. It is still not known what triggers relativistic jets in only a small fraction of AGN and thereby giving rise to the apparent radio-loud radio-quiet dichotomy (Ivezić et al. 2002; Cirasuolo et al. 2003). Both radio-loud and radio-quiet AGN may be categorized into several sub-classes such as Seyfert galaxies (Seyfert 1 and 2), radio galaxies, blazars comprising flat spectrum radio quasars (FSRQs) and BL Lac objects (BL Lacs) etc., According to the unification model, the observed differences between the different types of AGN are in part due to orientation effects (Antonucci 1993; Urry & Padovani 1995). One of the defining characteristics of AGN is that they show flux variations across the entire accessible electromagnetic spectrum (Wagner & Witzel 1995; Ulrich et al. 1997) over a wide range of timescales ranging from minutes to months and years. Though flux variations in AGN are known since their discovery, we still do not completely understand the physical processes that cause such variations (McHardy et al. 2006). Also, it is not unambiguously known if the same physical processes are responsible for the observed flux variations in different types of AGN. In spite of our lack of a clear knowledge on the cause of flux variations, this characteristic of AGN when probed particularly in the X-ray band can give important constraints on the physical properties in the innermost regions of AGN and can even provide clues on the observed radio-loud and radio-quiet dichotomy (Gliozzi et al. 2002).

Among the X-ray band, hard X-ray (with energies greater than 15 keV) variability in particular can provide clues about the physics of the central regions of AGN and kinematics of the jet as it is less affected by absorption than soft X-rays, when the line of sight hydrogen column density is less than 10^{23} cm^{-2} (Soldi et al. 2014). Hard X-rays can thus serve as an effective wavelength range to probe the intrinsic properties of the different classes of AGN. Therefore, the study of hard X-ray properties of the various types of AGN in general and hard X-ray flux variability in par-

* E-mail: priyanka@iiap.res.in

ticular can be used to test the validity of the unification model of AGN (Beckmann & Shrader 2012; Ghisellini et al. 1994; Urry & Padovani 1995). Various models are available in the literature on the physical processes that cause hard X-ray emission in AGN. According to Haardt & Maraschi (1993), the hard X-ray emission in radio-quiet AGN is due to the Comptonization of the soft accretion disk photons by a plasma of hot electrons situated above the disk. In the case of radio-loud AGN, in addition to the process that produces hard X-ray emission in radio-quiet AGN, there are additional contributions through inverse Compton (IC) processes from relativistic electrons in the jet.

In any given X-ray band, the observed characteristics of different types of AGN depend on the physical processes that contribute to the observed spectral energy distribution (SED) in that band. In blazars, the broad band SED shows two broad emission peaks: the low energy peak is produced by synchrotron emission and the high energy peak is produced by IC emission process. The seed photons for IC can be from various sources such as the synchrotron photons themselves (Konigl 1981), accretion disk (Dermer & Schlickeiser 1993; Boettcher et al. 1997), the broad line region (BLR, Sikora et al. 1994; Ghisellini & Madau 1996) or the torus (Błażejowski et al. 2000). These external photon fields contribute differently in individual blazars and this can explain the varied nature of the high energy component in the SED of blazars. Depending on the location of the synchrotron peak in their SEDs, blazars are further subdivided (Padovani & Giommi 1995; Abdo et al. 2010) into high synchroton peaked blazars (HSP, with synchrotron emission peaking at X-ray energies with $\nu_s > 10^{15}$ Hz), intermediate synchrotron peaked blazars (ISP, $10^{14} < \nu_s < 10^{15}$ Hz and low synchrotron peaked blazars (LSP, with synchrotron emission peaking in the IR; $\nu_s < 10^{14}$ Hz). In HSPs, the X-ray spectrum falls in the synchrotron region, thereby showing large amplitude X-ray variations at long as well as short time scales (Sembay et al. 1993; Tanihata et al. 2000; Zhang et al. 2002, 2005), however, less variable in the optical (Heidt 1996). On the other hand, LSPs are more variable in the optical (Heidt 1996) compared to the X-ray (Gupta et al. 2016) band which falls in the IC region of their SED. Nonetheless, it is not always the case and there are instances where the X-ray spectrum is found to have contribution both from the high energy tail of the synchrotron component and the IC component. This has been noticed in several LSP blazars (Tagliaferri et al. 2000; Tanihata et al. 2003; Wierzcholska & Wagner 2016) and in one HSP blazar (Kataoka & Stawarz 2016) namely Mrk 421.

Blazars are known to show fast variability. Detection of such fast variability time scales can set an upper limit on the size of the emission region as $R_s < \mathrm{c}\ \delta\ \mathrm{t}_{var}$, via light travel time arguments. Here, δ is the Doppler factor, and t_{var} is the variability time scale. Such fast time scale of variations (in the order of minutes) characterised by the flux doubling/halving time scale are often seen in high energy γ-rays (Aharonian et al. 2007; Gaidos et al. 1996). Also, in HSP blazars correlated X-ray and γ-ray variations are found (Baloković et al. 2016; Aleksić et al. 2015) which is very well expected in the one zone leptoinc model of blazar emission, wherein, both hard X-rays and γ-rays are produced by the same population of relativistic electrons in the jet. Detection of such short time scale X-ray flares with/without a high energy γ-ray counterpart will constrain the radiative processes operating in the sub-parsec scales of AGN. Detection of very small flux doubling/halving time scale is thus an important addition to the knowledge of AGN flux variability. Previous efforts to search for flux doubling/halving time scale < 15 minutes in the X-ray band were negative (Pryal et al. 2015). Therefore, any evidences for the presence of minute scale flux doubling/halving time scale is more important.

In the soft X-ray band, with X-rays having energies $<$ 10 keV, numerous results on the flux variability nature of AGN on time scales ranging from hours to months and years are available mainly based on observations from *Rossi X-ray Timing Explorer* (RXTE) and XMM-Newton (Nandra et al. 1997; Fiore et al. 1998; Turner et al. 1999; Uttley et al. 2002; Markowitz et al. 2003; Soldi et al. 2008; McHardy 2010). On the other hand, studies on the hard X-ray variability of AGN are very limited. They include hard X-ray spectral variability based on observations from BeppoSAX (Petrucci et al. 2000), INTEGRAL (Petrucci et al. 2013) and Suzaku (Reis et al. 2012). Long term hard X-ray monitoring observations have been recently possible owing to the observations by the Burst Alert Telescope (BAT; Barthelmy et al. 2005) instrument on board the *Swift* satellite (Gehrels et al. 2004). Because of *Swift*/BAT's observing capability in survey mode and its large field of view of $\sim$1.4 sr, we have long term monitoring data on a large sample of bright AGN from BAT. Using this data set, AGN have been studied for long term variability on time scale of days to years (Gehrels et al. 2004; Caballero-Garcia et al. 2012; Soldi et al. 2014). However, studies on the hard X-ray variations on time scales of the order of hours are available only on few individual objects such as Mrk 421 (Paliya et al. 2015) using the focusing hard X-ray telescope *Nuclear Spectroscopic Telescope Array* (*NuSTAR*; Harrison et al. 2013), sources such as BL Lac (Ravasio et al. 2003), ON 231 (Tagliaferri et al. 2000), Mrk 421 (Maraschi et al. 1999), Mrk 501 (Pian et al. 1998) etc. from BeppoSAX as well as observations from RXTE (Fossati et al. 2008). These observations pertaining to sources in different brightness states indicate different variability behaviour between hard and soft bands, which point to different physical processes contributing to the soft and hard X-ray emission.

Observations using NuSTAR with its high sensitivity and wide spectral coverage between $3 - 79$ keV is ideal to constrain the X-ray emission processes that contribute to the X-ray emission over a wide spectral range in AGN. We investigate here for the first time the hard X-ray flux variations on hourly time scales in the largest sample of AGN that includes both radio-loud and radio-quiet sources. The main motivation here is to understand (i) the similarities and differences in the flux variability nature of different types of AGN over a wide waveband of $3 - 79$ keV, (ii) the differences if any between flux variations in soft and hard X-ray bands and (iii) the presence of fast variations with flux doubling/halving time scale of few minutes. For this we use the publicly available data from observations by *NuSTAR*. The structure of the paper is as follows. In section 2, we describe the sample used and data reduction. In Section 3 we describe the various analysis carried out on the data set. We discuss our results in Section 4 and summarize the results in Section 5. We adopt a cosmology with $H_0 = 71$ km s^{-1} Mpc^{-1}, $\Omega_\Lambda = 0.73$ and $\Omega_m = 0.27$.

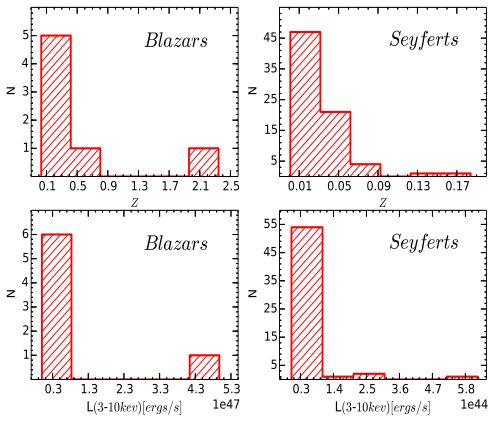

Figure 1. The distribution of redshift and the 3−10 keV luminosity of the sources. The left hand panels are for blazars, that includes FSRQs and BL Lacs, and the right hand panel are for Seyferts comprising Seyfert 1 and 2 galaxies.

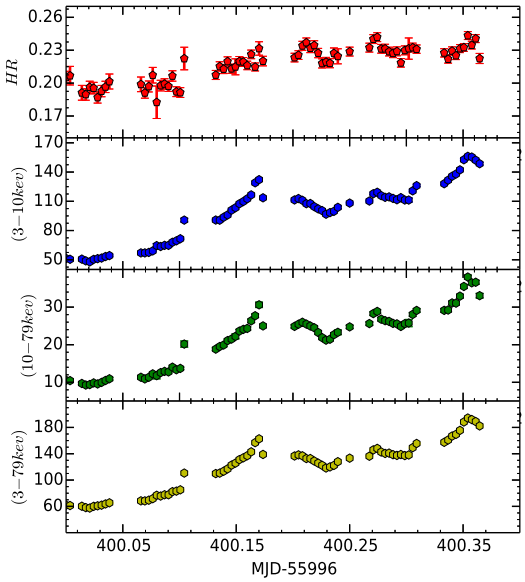

Figure 2. Light curves of the BL Lac object Mrk 421 corresponding to the observational ID 60002023031 and observed on 2013-04-14 for a duration of 15606 sec. From the top to the bottom are shown the HR variation, flux variations in the energy ranges of 3−10 keV (soft band), 10−79 keV (hard band) and 3−79 keV (total band) respectively. Each point corresponds to a binning of 300 seconds and the fluxes are in units of counts s^{-1}.

2 SAMPLE AND DATA REDUCTION

The goal of this work is to find the hard X-ray flux variations in different types of AGN. For this we have used the data from *NuSTAR*. *NuSTAR* (Harrison et al. 2013) launched in June 2012, is the first focusing hard X-ray telescope. It has a field of view 13′ x 13′. It consists of two co-aligned X-ray detector pairs with corresponding focal plane modules FPMA and FPMB[1]. *NuSTAR* observations of all AGN that have become public before March 2015 have been used in this work. Our sample thus consists of 81 AGN, among these 4 are BL Lacs, 3 are FSRQs, 24 are Seyfert 1 galaxies, 42 are Seyfert 2 galaxies and 8 are narrow line Seyfert 1 (NLSy1) galaxies. The details of the sources used in this study are given in Table 1. The distribution of redshifts and the 3−10 keV luminosity of the sources studied are shown in Figure 1 separately for radio-quiet sources and blazars.

Reduction of the NuSTAR data was done using the data analysis software *NuSTARDAS* v.1.4.1 distributed by the High Energy Astrophysics Archive Research Center (HEASARC). The calibrated, cleaned and screened event files were generated using the *nupipeline* task and using CALDB 20141107. A circular region of 60″ radius was taken to extract the source and background counts on the same detector. We extracted the 5 min binned light curves in the energy range of 3−79 keV in each focal plane module FPMA and FPMB using the *nuproducts* package available in *NuSTARDAS*. Further, these light curves were divided into two bands: 3−10 keV and 10−79 keV. To generate light curves, the count rates of the two modules FPMA and FPMB are combined using 'lcmath' task included in FTOOLS V.4.0. Sample light curves of the BL Lac object Mrk 421 are shown in Figure 2.

[1] https://heasarc.gsfc.nasa.gov/docs/nustar/

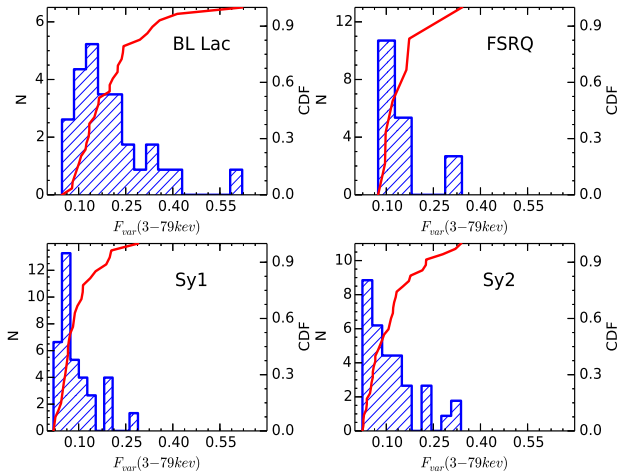

Figure 3. Histogram and cumulative distribution function (CDF) of $F_{\rm var}$ in the 3−79 keV band for different classes of AGN. The values of CDF are given in the right of each figure.

3 ANALYSIS

3.1 Variability Amplitude

To characterize the flux variations we used the fractional root mean square (rms) variability amplitude $F_{\rm var}$ (Edelson et al. 2002; Vaughan et al. 2003). This gives an estimate of the intrinsic variability amplitude relative to the mean count

Table 1. Information on the sources studied for flux variability. The quoted magnitudes are the V-band magnitudes taken from Véron-Cetty & Véron (2010) except for those appended with a * for which it is from NED (http://ned.ipac.caltech.edu/).

Name	α(2000)	δ(2000)	V (mag)	z	Type	Name	α(2000)	δ(2000)	V (mag)	z	Type
Mrk 335	00:06:19.5	+20:12:11	13.85	0.026	Sy1	3C 273	12:29:06.7	+02:03:08	12.85	0.158	FSRQ
NGC 424	01:11:27.7	−38:05:10	14.12	0.011	Sy2	3C 279	12:56:11.1	−05:47:22	17.75	0.538	FSRQ
NGC 513	01:24:26.8	+33:47:58	13.40	0.019	Sy2	Mrk 231	12:56:14.2	+56:52:25	13.84	0.041	Sy1
NGC 612	01:33:57.8	−36:29:36	13.20	0.030	Sy2	Mrk 248	13:15:17.2	+44:24:26	15.10	0.036	Sy2
MCG +01−05−047	01:52:49.0	−03:26:49	14.24	0.017	Sy2	MCG −06−30−15	13:35:53.4	−34:17:48	13.61	0.008	Sy1
NGC 788	02:01:06.5	−06:48:56	12.76	0.013	Sy2	NGC 5252	13:38:15.9	+04:32:33	14.21	0.022	Sy2
NGC 985	02:34:37.8	−08:47:15	14.28	0.043	Sy1	NGC 5273	13:42:08.3	+35:39:15	13.12	0.003	Sy2
NGC 1068	02:42:40.7	−00:00:47	10.83	0.003	Sy2	Mrk 273	13:44:42.1	+55:53:13	14.91	0.037	Sy2
1H 0323+342	03:24:41.2	+34:10:45	15.72	0.061	NLSy1	IC 4329A	13:49:19.3	−30:18:34	13.66	0.016	Sy1
NGC 1320	03:24:48.7	−03:02:32	14.00	0.009	Sy2	PKS 1409−651	14:13:09.8	−65:20:17	12.10	0.001	Sy2
NGC 1365	03:33:36.4	−36:08:24	12.95	0.006	Sy2	NGC 5506	14:13:14.8	−03:12:26	14.38	0.007	Sy1
3C 120	04:33:11.1	+05:21:15	15.05	0.033	Sy1	NGC 5548	14:17:59.6	+25:08:13	13.73	0.017	Sy1
MCG +03−13−01	04:46:29.7	+18:27:40	15.00	0.016	Sy2	NGC 5674	14:33:52.3	+05:27:30	13.70	0.025	Sy2
IRAS 04507+0358	04:53:25.7	+04:03:42	15.00	0.030	Sy2	Mrk 477	14:40:38.1	+53:30:16	15.03	0.038	Sy2
XSS J05054−2348	05:05:45.7	−23:51:14	17.00	0.035	Sy2	NGC 5728	14:42:23.9	−17:15:11	13.40	0.009	Sy2
ZW 468.002	05:08:19.7	+17:21:47	13.50	0.017	Sy2	IGR J14552−5133	14:55:17.8	−51:34:17	17.10	0.016	NLSy1
ARK 120	05:16:11.4	−00:09:00	13.92	0.033	Sy1	IC 4518A	14:57:41.2	−43:07:56	15.00	0.016	Sy2
IRAS 05189−2524	05:21:01.4	−25:21:45	14.75	0.042	Sy2	SWIFT J1514.5-8123	15:14:42.0	−81:23:38	∗17.3	0.068	Sy1
NGC 2110	05:52:11.4	−07:27:23	13.51	0.007	Sy2	Mrk 290	15:35:52.3	+57:54:09	15.30	0.030	Sy1
NGC 2273	06:50:08.7	+60:50:45	13.54	0.006	Sy2	Mrk 501	16:53:52.2	+39:45:36	13.78	0.033	BL Lac
1H 0707−495	07:08:41.5	−49:33:06	15.70	0.041	NLSy1	MCG +05−40−026	17:01:07.8	+29:24:25	15.78	0.036	NLSy1
IRAS 07245−3548	07:26:26.3	−35:54:22	16.80	0.029	Sy2	NGC 6300	17:16:59.2	−62:49:05	13.08	0.003	Sy2
Mrk 9	07:36:57.0	+58:46:13	14.37	0.039	Sy1	PDS 456	17:28:19.9	−14:15:56	14.03	0.184	NLSy1
IRAS 07378−3136	07:39:44.7	−31:43:02	∗16.8	0.025	Sy2	IGR J18244−5622	18:24:19.4	−56:22:09	14.40	0.017	Sy2
Mrk 1210	08:04:05.9	+05:06:50	13.70	0.013	Sy2	LEDA 3097193	18:26:32.4	+32:51:30	....	0.022	Sy2
FAIRALL 0272	08:23:01.1	−04:56:05	16.00	0.021	Sy2	3C 382	18:35:03.4	+32:41:47	15.39	0.058	Sy1
FAIRALL 1146	08:38:30.8	−35:59:33	16.10	0.031	Sy1	H 1834−653	18:38:20.5	−65:25:39	14.53	0.013	Sy2
SWIFT J0845.0−3531	08:45:21.4	−35:30:24	....	0.137	Sy1	3C 390.3	18:42:09.0	+79:46:17	15.38	0.057	Sy1
MCG +01−24−012	09:20:46.2	−08:03:21	13.70	0.020	Sy2	2E 1849.2−7832	18:57:07.7	−78:28:21	∗14.5	0.042	Sy1
MCG +04−22−042	09:23:43.1	+22:54:33	14.80	0.033	NLSy1	IGR J19473+4452	19:47:19.4	+44:49:42	15.70	0.053	Sy2
MCG −05−23−16	09:47:40.2	−30:56:54	13.69	0.008	Sy1	3C 403	19:52:15.9	+02:30:24	16.50	0.059	Sy2
3C 227	09:47:45.1	+07:25:20	16.97	0.086	Sy1	MCG +07−41−003	19:59:28.3	+40:44:02	15.10	0.056	Sy2
NGC 3079	10:01:58.5	+55:40:50	12.18	0.004	Sy2	IGR J20187+4041	20:18:38.7	+40:41:00	....	0.014	Sy2
Mrk 728	11:01:01.8	+11:02:50	16.93	0.036	Sy2	IC 5063	20:52:02.2	−57:04:08	13.60	0.011	Sy2
Mrk 421	11:04:27.2	+38:12:32	12.90	0.031	BL Lac	IGR J21277+5656	21:27:44.9	+56:56:40	18.79	0.014	NLSy1
NGC 3516	11:06:47.4	+72:34:07	12.40	0.009	Sy1	IRAS F21318−2739	21:34:45.1	−27:25:55	∗16.36	0.067	Sy1
Mrk 732	11:13:49.8	+09:35:10	14.17	0.030	Sy1	PKS 2149−306	21:51:55.4	−30:27:54	17.90	2.345	FSRQ
NGC 4051	12:03:09.6	+44:31:53	12.92	0.002	NLSy1	PKS 2155−304	21:58:52.0	−30:13:32	13.09	0.116	BL Lac
NGC 4151	12:10:32.5	+39:24:21	11.85	0.003	Sy1	BL Lac	22:02:43.3	+42:16:39	14.72	0.069	BL Lac
WAS 49b	12:14:17.8	+29:31:43	15.40	0.064	Sy2	NGC 7582	23:18:23.5	−42:22:14	13.57	0.005	Sy1
NGC 4395	12:25:48.9	+33:32:48	10.27	0.001	Sy2						

rate exceeding the measurement noise in the light curves. $F_{\rm var}$ is defined as

$$F_{\rm var} = \sqrt{\frac{S^2 - \bar{\sigma^2}_{\rm err}}{\bar{x}^2}} \quad (1)$$

where S^2 is the sample variance, $\bar{x}$ is the arithmetic mean of x_i and $\bar{\sigma^2}_{\rm err}$ represents the mean square error, given by

$$S^2 = \frac{1}{N-1}\sum_{i=1}^{N}(x_i - \bar{x})^2 \quad (2)$$

$$\bar{\sigma^2}_{\rm err} = \frac{1}{N}\sum_{i=1}^{N}\sigma^2_{\rm err,i} \quad (3)$$

The uncertainty in $F_{\rm var}$ is given by

$$err(F_{\rm var}) = \sqrt{\left(\sqrt{\frac{1}{2N}}\frac{\bar{\sigma^2}_{\rm err}}{\bar{x}^2 F_{\rm var}}\right)^2 + \left(\sqrt{\frac{\bar{\sigma^2}_{\rm err}}{N}}\frac{1}{\bar{x}}\right)^2} \quad (4)$$

$F_{\rm var}$ and $err(F_{\rm var})$ were calculated for each binned light curve. Variability analysis of the sample was carried out in soft (3−10 keV), hard (10−79 keV) and total (3−79 keV) bands. An object is considered variable if $F_{\rm var}$ (significant at 1 σ) is greater than zero. Calculated values of $F_{\rm var}$ for sources that are found to be variable are given in Tables 2, 3 , 4, 5 and 6 for BL Lacs, FSRQs, Seyfert 1 galaxies, Seyfert 2 galaxies and NLSy1 galaxies respectively. About 65% of the sources in our sample are found to be variable.

The number of BL Lacs, FSRQs and NLSy1 galaxies studied here is small (compared to Seyfert 1 and 2 galaxies) to consider the variability shown by these objects as a representation of their class as a whole. Nevertheless, we calculated the weighted mean variability of the different classes of AGN in different X-ray bands namely soft, hard and total bands and the results are presented in Table 7. In the total NuSTAR band we find an average $F_{\rm var}$ of 0.310 ± 0.138 and 0.093 ± 0.047 for BL Lacs and FSRQs respectively. In the radio-quiet category, the average $F_{\rm var}$ values for Seyfert 1 and Seyfert 2 galaxies are 0.092 ± 0.061 and 0.149 ± 0.108 respectively. The histogram and cumulative distribution of $F_{\rm var}$ in the total band for different classes of AGN are shown in Figure 3.

To check for the robustness of the differences in the weighted mean $F_{\rm var}$ values of different classes of AGN, we carried out two non-parametric statistical tests, namely the Mann-Whitney U test (hereafter referred to as the U test)

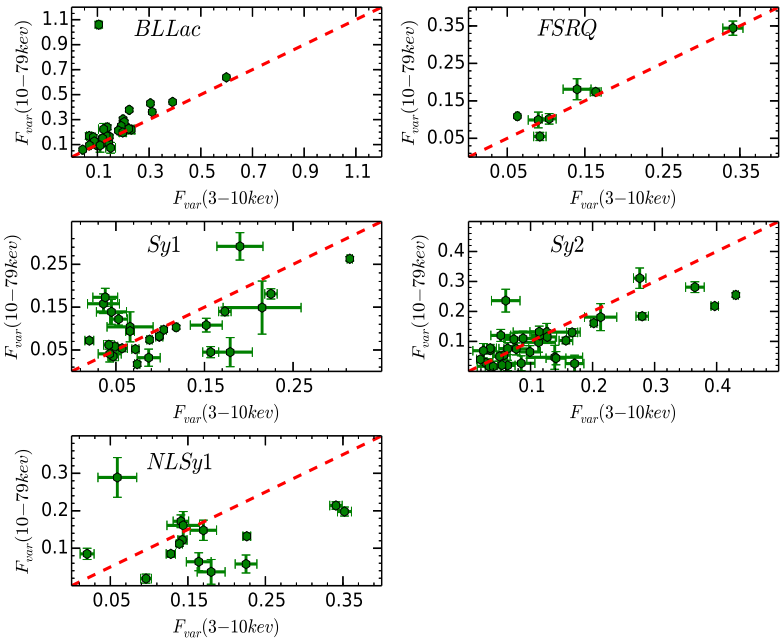

Figure 4. Correlation of flux variations between soft and hard bands for the different classes of AGN. The dashed lines have a slope of unity and indicate identical variation of $F_{\rm var}$ values between soft and hard bands.

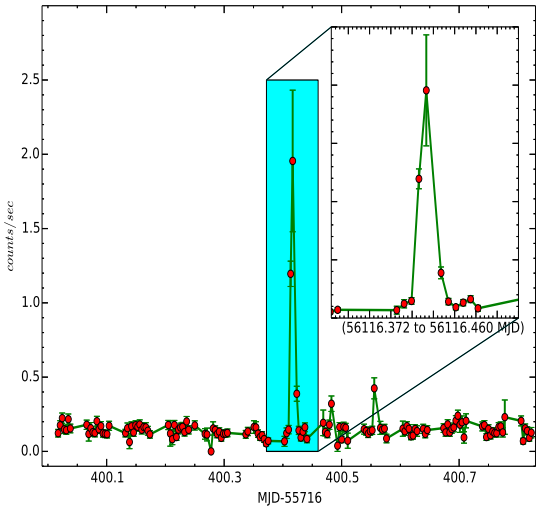

Figure 5. NuSTAR light curve of the BL Lac PKS 2155−304 in the energy range 10−79 keV. The inset shows the zoomed in section of the light curve around MJD 56116.372 to 56116.460 where the shortest doubling time of 1.65 ± 0.16 is observed.

and the Kolmogorov-Smirnov test (hereafter referred to as the KS test). The U-test is based on the rank of observations rather than the observations themselves. It allows two groups or conditions to be compared without making the assumption that the values are normally distributed. The null hypothesis that is tested in U-test is that the distribution of $F_{\rm var}$ values of any two classes of AGN (or between different energy bands in a particular class of AGN) that is compared is identical. The null hypothesis is rejected (at a particular level of confidence) if the U-statistics is less than the critical U-value ($U_{\rm crit}$). The KS test similar to the U-test is also a non-parametric test that can determine if two data sets differ significantly. In this statistics the cumulative distribution of the two data sets that is to be tested are plotted and KS test uses the maximum vertical deviation between the two curves to give the statistics D. The null hypothesis here is that the two data sets that are compared are from the same distribution. This null hypothesis is rejected if D is greater than the critical D value ($D_{\rm crit}$). The critical values $U_{\rm crit}$ and $D_{\rm crit}$ are evaluated at the 5% confidence level. In Table 8 we give the results of the two test statistics along with their corresponding P values for the various comparisons that are studied for the different classes of AGN. From Table 8 it is evident that both U and KS tests reject the null hypothesis of any differences in the variability properties between FSRQs-BL Lacs and Sy1-Sy2 galaxies in soft, hard and total energy bands. However, comparing Seyfert galaxies (including Seyfert 1 and 2) and blazars (that include FSRQs and BL Lacs), statistical tests clearly indicate that the blazar sources in our sample are more variable than Seyfert galaxies, in all the three energy bands investigated here, namely soft, hard and the full NuSTAR band.

3.2 Flux variations between soft and hard bands

To compare the relation between flux variations in the soft (3−10 keV) and hard (10−79 keV) X-ray bands, $F_{\rm var}$ was evaluated for the variable sources in the soft and hard bands. In general, for the different types of AGN studied in this work, the derived values of $F_{\rm var}$ do not show an one to one correspondence between the two energy bands as evident from Figure 4. In the case of BL Lac objects, we have a total of 30 sets of observations on 3 objects. Considering these observations in total, we find that for 90% of the ob-

Table 2. Characteristics of flux variations of BL Lac objects

Name	Type	OBS ID	Obs. date	Exposure (secs)	$F_{\rm var} \pm err(F_{\rm var})$ 3−10 keV	10−79 keV	3−79 keV
Mrk 421	BL Lac	10002015001	2012-07-07	42034	0.209±0.003	0.247±0.008	0.225±0.004
		10002016001	2012-07-08	24885	0.305±0.003	0.430±0.009	0.358±0.004
		60002023002	2013-01-02	9152	0.068±0.010	0.168±0.027	0.088±0.013
		60002023004	2013-01-10	22633	0.119±0.008	0.146±0.021	0.132±0.010
		60002023006	2013-01-15	24182	0.199±0.004	0.302±0.012	0.243±0.005
		60002023008	2013-01-20	24968	0.084±0.007	0.159±0.020	0.095±0.009
		60002023010	2013-02-06	19307	0.097±0.005	0.095±0.014	0.108±0.006
		60002023012	2013-02-12	14780	0.204±0.005	0.280±0.012	0.241±0.006
		60002023014	2013-02-16	17359	0.231±0.013	0.220±0.034	0.237±0.020
		60002023016	2013-03-04	17252	0.122±0.005	0.115±0.016	0.122±0.007
		60002023018	2013-03-11	17474	0.144±0.005	0.112±0.014	0.125±0.006
		60002023020	2013-03-17	16558	0.088±0.004	0.125±0.012	0.102±0.006
		60002023022	2013-04-02	24772	0.223±0.004	0.378±0.011	0.295±0.006
		60002023024	2013-04-10	5758	0.146±0.005	0.164±0.013	0.165±0.006
		60002023025	2013-04-11	57509	0.599±0.001	0.638±0.004	0.621±0.002
		60002023027	2013-04-12	7630	0.134±0.002	0.172±0.005	0.150±0.002
		60002023029	2013-04-13	16510	0.221±0.002	0.226±0.005	0.224±0.002
		60002023031	2013-04-14	15606	0.312±0.001	0.361±0.002	0.335±0.001
		60002023033	2013-04-15	17278	0.192±0.006	0.248±0.005	0.199±0.008
		60002023035	2013-04-16	20279	0.391±0.002	0.441±0.004	0.414±0.002
		60002023037	2013-04-18	17795	0.181±0.005	0.212±0.013	0.199±0.006
		60002023039	2013-04-19	15958	0.120±0.005	0.149±0.013	0.134±0.006
Mrk 501	BL Lac	60002024004	2013-05-08	26141	0.138±0.007	0.238±0.019	0.163±0.008
		60002024006	2013-07-12	10857	0.043±0.004	0.059±0.008	0.047±0.005
		60002024008	2013-07-13	10343	0.069±0.007	0.094±0.012	0.081±0.007
PKS 2155−304	BL Lac	10002010001	2012-07-08	33838	0.105±0.008	1.060±0.027	0.319±0.011
		60002022004	2013-07-16	13856	0.124±0.020	0.223±0.046	0.134±0.022
		60002022008	2013-08-08	13496	0.110±0.040	0.093±0.054	0.156±0.054
		60002022012	2013-08-26	11356	0.198±0.013	0.197±0.030	0.209±0.015
		60002022014	2013-09-04	12282	0.151±0.019	0.074±0.043	0.079±0.024

Table 3. Characteristics of flux variations of FSRQs

Name	Type	OBS ID	Obs.date	Exposure (secs)	$F_{\rm var} \pm err(F_{\rm var})$ 3−10 keV	10−79 keV	3−79 keV
3C 273	FSRQ	00015013001	2012-07-02	2573	0.341±0.013	0.344±0.019	0.341±0.012
		00015016001	2012-07-02	2990	0.140±0.018	0.181±0.028	0.164±0.017
		10002020001	2012-07-14	244003	0.063±0.002	0.109±0.002	0.074±0.002
		10012007001	2012-07-13	4530	0.090±0.013	0.099±0.021	0.096±0.013
3C 279	FSRQ	60002020002	2013-12-16	39594	0.104±0.009	0.102±0.014	0.098±0.009
		60002020004	2013-12-31	42810	0.164±0.007	0.174±0.010	0.173±0.006
PKS 2149−306	FSRQ	60001099004	2014-04-18	44167	0.092±0.008	0.055±0.011	0.120±0.007

servations, the amplitude of variations in the hard band is larger than the variations in the soft band. The weighted mean $F_{\rm var}$ for BL Lac objects in the hard and soft bands are 0.340 ± 0.144 and 0.342 ± 0.177 respectively. Statistical analysis by both U and KS tests provides no evidence to suggest the variability pattern between soft and hard bands in BL Lacs are different. FSRQs too show similar amplitude of variations within the errors between hard and soft bands and have weighted mean $F_{\rm var}$ of 0.112 ± 0.028 and 0.079 ± 0.045 in hard and soft bands respectively. Among the 28 sets of observations on 17 Seyfert 1 galaxies, in about 36% of observations the amplitude of flux variations in the hard band are larger than those in the soft band. Similarly, in Seyfert 2 galaxies in 13/36 sets of observations, the hard band shows a higher variability amplitude compared to the soft band. However, based on statistical analysis (Table 8) we find no difference in the variability characteristics between soft and hard bands in Seyfert 1 and 2 galaxies. For NLSy1 galaxies, we have 14 sets of observations on 7 objects. Considering all the 7 objects together, both U and KS tests show that there is no significant difference in the $F_{\rm var}$ values between soft and hard bands. Of these, we find that in 3 sets of ob-

servations ($\sim 20\%$) the variability amplitude is larger in the hard band than in the soft band pertaining to the sources 1H0323+342, MCG +04−22−042 and PDS 456.

3.3 Flux variability time scale

Knowledge of the time scales on which the X-ray flux varies is very important as it can put constraints on the size of the emission region. For sources that have shown flux variations, we scan their light curves in the energy range 3−10 keV and 10−79 keV to find the time scale of flux variations. For this we calculated the flux doubling time/halving time defined as

$$F(t) = F(t_0) \cdot 2^{(t-t_0)/\tau} \quad (5)$$

here, τ is the characteristic flux doubling/halving time scale and $F(t_0)$ and $F(t)$ are values of the fluxes at time t_0 and t respectively. This time scale is evaluated by imposing the condition that the difference between the fluxes at times t_0 and t is greater than 3σ (Foschini et al. 2011). The best fit values obtained on fitting Equation 5 to the data are given in Table 9. The quoted uncertainties in τ are the 1 σ errors. A total of 13 sources are found to have flux doubling/halving time scale less than 10 min. Such behaviour is not restricted to one AGN type and is seen in all types of AGN. Among the Seyfert 2 galaxies NGC 1365 has shown flux doubling/halving time less than 10 min in all three epochs it has been observed. The shortest flux doubling/halving time scale measured in the energy range of 10−79 keV is 1.65 ± 0.16 min for the BL Lac object PKS 2155−304. The 10−79 keV light curve of the source is shown in Figure 5 and the part of the light curve during the epoch where such doubling time is observed is shown in the inset in Figure 5. This is significantly smaller than that previously observed in the X-ray band (Paliya et al. 2015) in another blazar Mrk 421 and is the shortest flux doubling/halving time in the hard X-ray band ever recorded in PKS 2155−304.

3.4 Time delay between flux variations in hard and soft bands

To quantify the degree of correlation between flux variations in soft and hard bands we used a model based approach using the code JAVELIN [2], a Python based implementation of SPEAR (Stochastic Process Estimation for AGN Reverberation; Zu et al. 2011, 2013). JAVELIN has been designed to improve lag measurements between continuum and line variations in AGN by modelling the light curves using a damped random walk process (DRWP; Kelly et al. 2009; MacLeod et al. 2010). It then compares the simulated light curves with the observed ones to find the lag and this has been found to work well (Pancoast et al. 2014). We applied the JAVELIN method to all the sources in our sample. For all the sources the variations between soft and hard bands are consistent with zero lag. Several studies do exist in the literature on time lags between flux variations in different X-ray bands. For blazars in general using data in the 0.3− 10 keV band, soft lags (lower energy variations lagging the higher energy variations), hard lags (higher energy variations lagging the lower energy variation) and zero lags have been observed (Falcone et al. 2004; Zhang et al. 2006; Brinkmann et al. 2003; Ravasio et al. 2004; Abeysekara et al. 2016). This indicates the complex spectral and temporal characteristics of blazars that show different behaviour at different times. Observations of few Seyfert galaxies in the hard X-ray band by SWIFT/BAT in 2 days binned light curve did not show any delay between 20−50 and 50−100 keV bands (Caballero-Garcia et al. 2012).

3.5 Duty cycle of flux variations

To characterize the incidence of observability of X-ray variations in different classes of AGN, we have calculated the duty cycle of X-ray flux variations using the definition of Romero et al. (1999). Since only about 65% of the sources in our sample has shown variations exceeding the measurement noise characterised by $F_{\rm var}$, duty cycles are estimated not as a fraction of the variable objects within a given class, but as the ratio of the time over which the objects of a given class are found to vary to the total time of observations carried out on each objects in the class. An approach of this kind will take into account the fact that all AGN do not show variations at all times. Also, as the duration of observation is not the same for all the objects, the contribution to the duty cycle has been weighted by the number of times, as well as the duration each source was observed. Duty cycle is defined as

$$DC = \frac{\sum_{i=1}^{n} N_i(1/\Delta t_i)}{\sum_{i=1}^{n}(1/\Delta t_i)} \times 100\% \quad (6)$$

Here, $\Delta t_i = \Delta t_0(1+z)^{-1}$, is the duration corrected for cosmological redshift of the source observed and N_i equals 1 if the object is variable during the period of observations Δt_i and 0 otherwise. We find NLSy1 galaxies show the highest DC of 87.14% followed by BL Lacs (82.44 %), Seyfert galaxies (Seyfert 1 and 2 galaxies show similar DC of variability of 55.87 % and 56.47% respectively) and FSRQs (22.79%). Most of the BL Lacs belong to the HSP category of AGN and FSRQs are in general LSP sources. In the X-ray band, HSPs are known to be more variable in the X-ray band than LSPs, because, in the former the X-ray spectrum falls in the synchrotron region of the SED, while in the latter, it falls in the IC region. Therefore, the difference in the DC of variability between BL Las and FSRQs is due to the differences in the physical processes that contribute to the X-ray emission in the NuSTAR band in these two classes of AGN.

3.6 Spectral variations

The lack of one to one correspondence between the amplitude of flux variations in the soft and hard bands in some sources indicate that they show spectral variations. To further characterise spectral variations, we construct diagrams of hardness ratio (HR) plotted as a function of total flux in the 3−79 keV energy range. This is a model independent way to study spectral variations. HR is estimated using the following relation

$$HR = \frac{F_{hard}}{F_{soft}} \quad (7)$$

[2] http://www.astronomy.ohio-state.edu/ yingzu/codes.html

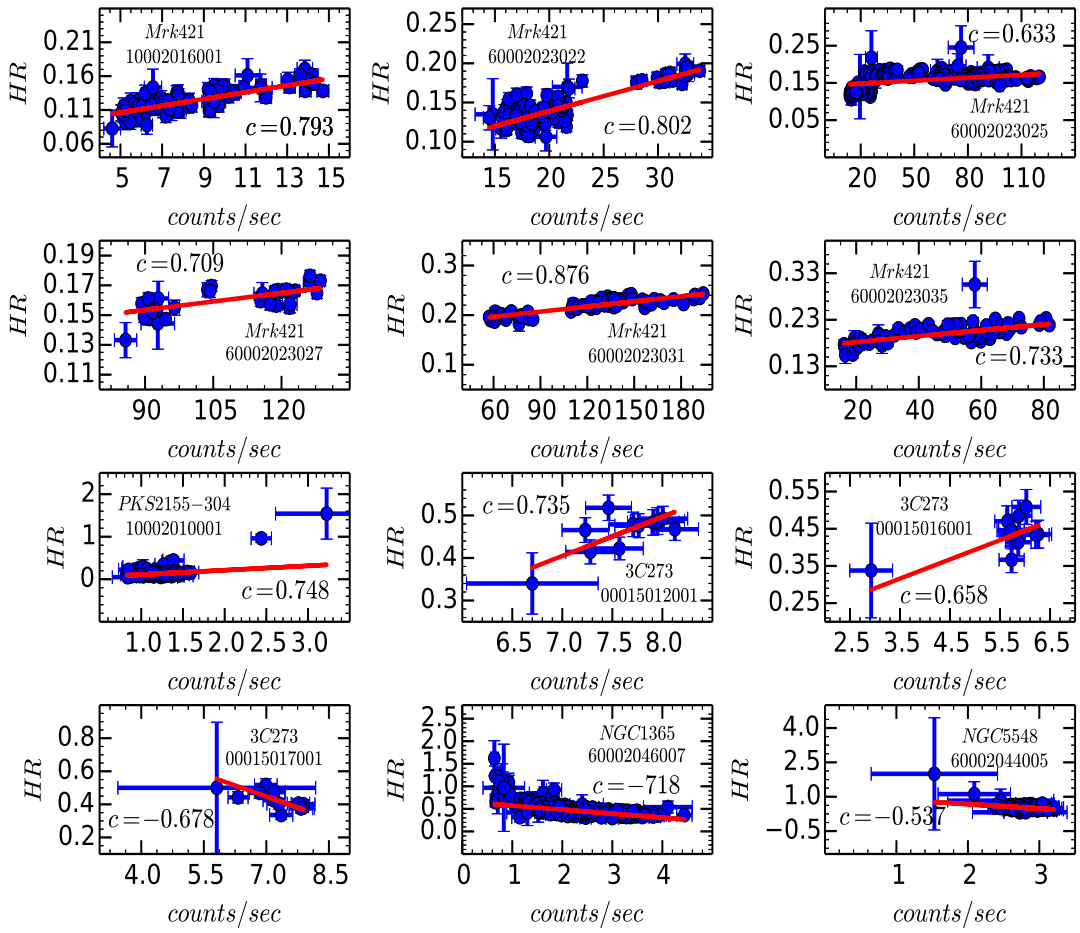

Figure 6. Hardness ratio plotted as a function of count rate in the 3−79 keV energy range. Red solid line is the weighted linear least squares fit to the data. The name of the source, the OBSID and the correlation coefficient are given in each panel.

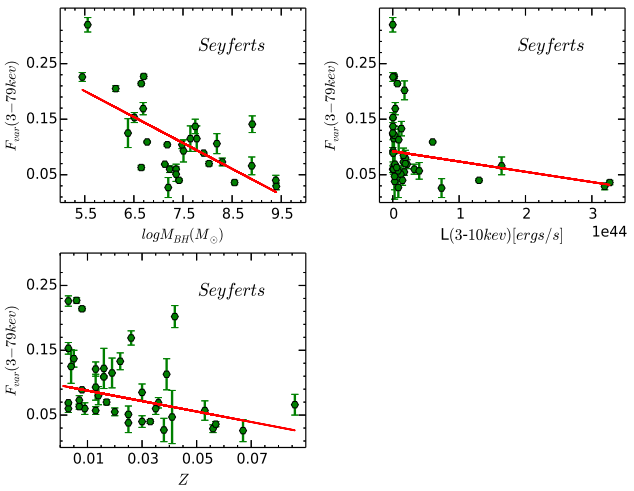

Figure 7. Correlation of $F_{\rm var}$ with BH mass, redshift and luminosity in the 3−10 keV band.

where, F_{hard} and F_{soft} refer to the fluxes in the 10−79 keV and the 3−10 keV respectively. For most of the sources we do not find a significant correlation between variations in HR and total flux. However, for some sources we do find a correlation. For those sources, the plot of HR as a function of the flux in the 3−79 keV band is shown in Figure 6. To quantify the significance of the correlation, we fit the observed points in the HR v/s flux diagram using a linear function of the form $HR = a \times flux_{3-79keV} + b$. During the fit we take into account the errors both in HR and flux following Press et al. (1992). The results of the fit are given in Table 10 and they are shown as solid lines in Figure 6. Significant spectral variations are seen in the BL Lacs objects Mrk 421 and PKS 2155−304, the FSRQ 3C 273, the Seyfert 1 galaxy NGC 5548 and the Seyfert 2 galaxy NGC 1365. For the BL Lac object Mrk 421 a significant harder when brighter trend is seen in 6 epochs of observations. However, for the FSRQ 3C 273, in the three epochs where a correlation between HR and total flux is found, on two epochs a harder when brighter trend is found, while, in one epoch a softer when brighter trend is noticed. Blazars in general are found to show a harder when brighter behaviour. Such hardening when brightening behaviour more often seen in the HSP category (Giommi et al. 1990; Pian et al. 1998;

Table 4. Characteristics of flux variations of Seyfert 1 galaxies

Name	Type	OBS ID	Obs.date	Exposure (secs)	$F_{\rm var} \pm err(F_{\rm var})$ 3−10 keV	10−79 keV	3−79 keV
Mrk 335	Sy1	60001041002	2013-06-13	21299	0.190±0.026	0.292±0.032	0.204±0.022
		60001041003	2013-06-13	21525	0.179±0.025	0.045±0.034	0.188±0.023
		60001041005	2013-06-25	93028	0.157±0.009	0.045±0.013	0.114±0.008
3C 120	Sy1	60001042002	2013-02-06	21606	0.047±0.006	0.035±0.010	0.036±0.006
		60001042003	2013-02-06	127731	0.074±0.003	0.017±0.005	0.044±0.003
Mrk 9	Sy1	60061326002	2013-10-29	23310	0.066±0.026	0.104±0.035	0.113±0.024
MCG −05−23−16	Sy1	10002019001	2012-07-16	33927	0.088±0.003	0.074±0.005	0.082±0.003
		60001046002	2013-06-03	160478	0.104±0.003	0.097±0.005	0.096±0.003
3C 227	Sy1	60061329004	2014-02-26	12064	0.036±0.018	0.158±0.023	0.066±0.016
NGC 3516	Sy1	60002042004	2014-07-11	72089	0.053±0.010	0.122±0.014	0.060±0.009
Mrk 732	Sy1	60061208002	2013-06-11	26359	0.043±0.013	0.041±0.019	0.085±0.013
NGC 4151	Sy1	60001111002	2012-11-12	21864	0.049±0.003	0.058±0.004	0.050±0.002
		60001111003	2012-11-12	57036	0.099±0.004	0.081±0.003	0.069±0.003
		60001111005	2012-11-14	61531	0.099±0.002	0.082±0.003	0.088±0.002
Mrk 231	Sy1	60002025004	2013-05-09	28557	0.215±0.044	0.149±0.062	0.047±0.041
MCG −06−30−15	Sy1	60001047002	2013-01-29	23270	0.225±0.007	0.181±0.012	0.199±0.007
		60001047003	2013-01-30	127232	0.314±0.003	0.263±0.005	0.289±0.003
		60001047005	2013-02-02	29646	0.173±0.007	0.140±0.010	0.154±0.006
NGC 5506	Sy1	60061323002	2014-04-01	56585	0.072±0.004	0.052±0.006	0.063±0.004
NGC 5548	Sy1	60002044006	2013-09-10	51460	0.066±0.005	0.094±0.007	0.066±0.005
		60002044008	2013-12-20	50103	0.057±0.006	0.054±0.008	0.073±0.006
Mrk 290	Sy1	60061266002	2013-11-14	25012	0.087±0.013	0.032±0.020	0.023±0.013
		60061266004	2013-11-27	26348	0.038±0.014	0.173±0.021	0.057±0.013
3C 390.3	Sy1	60001082002	2013-05-24	23643	0.042±0.006	0.062±0.010	0.053±0.006
		60001082003	2013-05-24	47559	0.020±0.005	0.072±0.007	0.020±0.005
IRAS F21318−2739	Sy1	60061306002	2013-10-22	19809	0.045±0.017	0.139±0.029	0.026±0.017
NGC 7582	Sy1	60061318002	2012-08-31	16463	0.152±0.018	0.108±0.016	0.137±0.013
IC 4329A	Sy1	60001045002	2012-08-12	162399	0.118±0.002	0.103±0.004	0.109±0.002

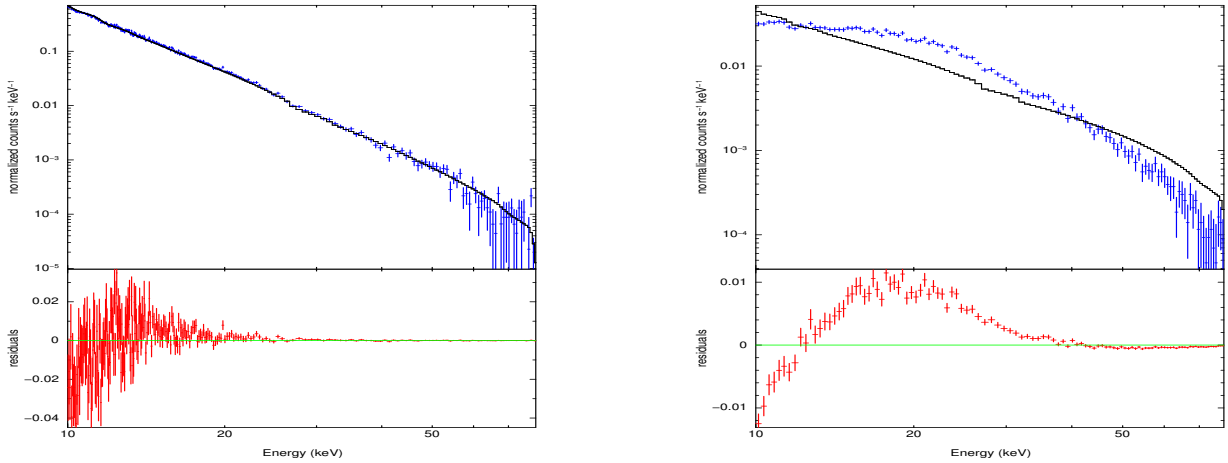

Figure 8. Hard X-ray spectrum of the BL Lac Mrk 421 (left) and the Seyfert 1 galaxy PKS 1409−651 (right) fitted with a power law model along with the residuals.

Giommi et al. 1990; Pian et al. 1998) among other things could be due to the shift of their broad band SEDs to higher energies (Brinkmann et al. 2003). The behaviour seen in Mrk 421 here is observed before as well (Takahashi et al. 1996). For the source PKS 2155−304 too, we find a hardening when brightening trend, also noted earlier in XMM observations (Zhang et al. 2006). In the radio-quiet category, two Seyfert galaxies, namely NGC 5548 and NGC 1365 showed spectral variations with their spectra becoming softer with increasing brightness. This trend is also known in other Seyfert galaxies based on observations from RXTE (Sobolewska & Papadakis 2009), Swift/XRT (Connolly et al. 2016) and Swift/BAT (Caballero-Garcia et al. 2012), which is expected in various models (Haardt et al. 1997; Turner & Miller 2009). We con-

Table 5. Characteristics of flux variations of Seyfert 2 galaxies

Name	Type	OBS ID	Obs.date	Exposure (secs)	$F_{\rm var} \pm err(F_{\rm var})$ 3−10 keV	10−79 keV	3−79 keV
NGC 513	Sy2	60061012002	2013-02-16	16040	0.113±0.027	0.097±0.033	0.115±0.023
NGC 788	Sy2	60061018002	2013-01-28	15411	0.088±0.031	0.110±0.024	0.093±0.020
NGC 1068	Sy2	60002030002	2012-12-18	57851	0.057±0.010	0.054±0.013	0.027±0.008
		60002030004	2012-12-20	48560	0.035±0.010	0.071±0.013	0.065±0.009
		60002030006	2012-12-21	19461	0.052±0.016	0.120±0.020	0.087±0.013
NGC 1365	Sy2	60002046002	2012-07-25	36258	0.276±0.010	0.311±0.034	0.215±0.019
		60002046003	2012-07-26	40588	0.157±0.011	0.103±0.011	0.130±0.008
		60002046005	2012-12-24	66297	0.202±0.005	0.161±0.007	0.172±0.004
		60002046007	2013-01-23	73650	0.431±0.004	0.255±0.007	0.338±0.004
		60002046009	2013-02-12	69877	0.397±0.006	0.218±0.009	0.280±0.006
MCG +03−13−01	Sy2	60061051002	2014-03-18	20088	0.139±0.045	0.047±0.040	0.122±0.031
XSS J05054−2348	Sy2	60061056002	2013-08-21	21161	0.035±0.010	0.077±0.013	0.060±0.009
IRAS 05189−2524	Sy2	60002027002	2013-02-20	23141	0.060±0.023	0.236±0.038	0.177±0.023
		60002027004	2013-10-02	25370	0.213±0.026	0.181±0.045	0.227±0.025
NGC 2110	Sy2	60061061004	2013-02-14	12019	0.028±0.008	0.028±0.011	0.073±0.007
IRAS 07378−3136	Sy2	60061351002	2014-04-20	23952	0.077±0.020	0.075±0.020	0.038±0.015
Mrk 1210	Sy2	60061078002	2012-10-05	15447	0.115±0.014	0.120±0.015	0.121±0.011
MCG +01−24−012	Sy2	60061091002	2013-04-03	12376	0.063±0.014	0.076±0.020	0.048±0.013
		60061091004	2013-04-10	9386	0.141±0.016	0.044±0.022	0.111±0.014
		60061091006	2013-04-18	12178	0.171±0.015	0.026±0.028	0.053±0.016
		60061091010	2013-05-12	15334	0.050±0.011	0.050±0.016	0.024±0.010
		60061091012	2013-05-22	12289	0.063±0.012	0.020±0.017	0.038±0.011
NGC 3079	Sy2	60061097002	2013-11-12	21542	0.126±0.054	0.131±0.029	0.125±0.026
NGC 4395	Sy2	60061322002	2013-05-10	19249	0.365±0.015	0.281±0.018	0.320±0.013
Mrk 248	Sy2	60061241002	2013-04-21	12901	0.033±0.019	0.017±0.025	0.036±0.017
		60061241004	2013-11-17	28909	0.040±0.013	0.016±0.018	0.065±0.011
		60061241006	2013-11-23	23056	0.127±0.015	0.115±0.022	0.107±0.014
NGC 5273	Sy2	60061350002	2014-07-14	21119	0.167±0.009	0.130±0.013	0.153±0.009
NGC 5674	Sy2	60061337002	2014-07-10	20671	0.073±0.014	0.107±0.021	0.051±0.013
Mrk 477	Sy2	60061255002	2014-05-15	18076	0.085±0.022	0.027±0.025	0.027±0.018
NGC 6300	Sy2	60061277002	2013-02-25	17706	0.280±0.010	0.184±0.012	0.226±0.008
LEDA 3097193	Sy2	60061354002	2014-05-19	15645	0.114±0.015	0.132±0.019	0.133±0.013
H 1834−653	Sy2	60061288002	2013-02-24	27391	0.054±0.007	0.021±0.009	0.057±0.006
IGR J19473+4452	Sy2	60061292002	2012-11-06	18214	0.024±0.017	0.069±0.024	0.057±0.015
MCG +07−41−003	Sy2	60001083004	2013-03-01	20715	0.019±0.006	0.040±0.009	0.029±0.006
IGR J20187+4041	Sy2	60061297002	2013-12-21	20967	0.099±0.017	0.065±0.021	0.080±0.014

Table 6. Characteristics of flux variations of NLSy1 galaxies

Name	Type	OBS ID	Obs.date	Exposure (secs)	$F_{\rm var} \pm err(F_{\rm var})$ 3−10 keV	10−79 keV	3−79 keV
1H 0323+342	NLSy1	60061360002	2014-03-15	101633	0.141±0.010	0.172±0.017	0.138±0.010
MCG +04−22−042	NLSy1	60061092002	2012-12-26	18845	0.020±0.009	0.085±0.015	0.081±0.009
NGC 4051	NLSy1	60001050002	2013-06-17	9434	0.225±0.014	0.058±0.024	0.168±0.014
		60001050003	2013-06-17	45737	0.341±0.006	0.214±0.010	0.277±0.006
		60001050005	2013-10-09	10202	0.164±0.016	0.064±0.024	0.128±0.015
		60001050006	2013-10-09	49621	0.352±0.009	0.198±0.012	0.273±0.008
		60001050008	2014-02-16	56683	0.226±0.005	0.132±0.009	0.180±0.005
IGR J14552−5133	NLSy1	60061259002	2013-09-19	21943	0.170±0.017	0.148±0.027	0.160±0.017
MCG +05−40−026	NLSy1	60061276002	2013-12-19	20999	0.147±0.019	0.111±0.029	0.073±0.018
PDS 456	NLSy1	60002032010	2014-02-26	109717	0.144±0.020	0.161±0.037	0.180±0.022
IGR J21277+5656	NLSy1	60001110002	2012-11-04	49202	0.143±0.006	0.122±0.010	0.138±0.006
		60001110003	2012-11-05	28765	0.096±0.007	0.019±0.012	0.054±0.007
		60001110005	2012-11-06	74583	0.139±0.004	0.112±0.007	0.124±0.004
		60001110007	2012-11-08	42110	0.128±0.006	0.085±0.009	0.101±0.006

Table 7. Weighted mean variability characteristics of different classes of AGN. N1 and N2 represent the number of objects and the number of observations respectively.

Type	N1	N2	avg($F_{\rm var} \pm err(F_{\rm var})$)		
			3−10 keV	10−79 keV	3−79 keV
BL_Lac	3	30	0.342±0.177	0.340±0.144	0.310±0.138
FSRQ	3	7	0.079±0.045	0.112±0.028	0.093±0.047
Sy1	17	28	0.108±0.068	0.089±0.052	0.092±0.061
Sy2	23	36	0.191±0.156	0.120±0.082	0.149±0.108
NLSy1	7	14	0.177±0.085	0.122±0.052	0.151±0.065
LSP	3	7	0.079±0.045	0.112±0.028	0.093±0.047
HSP	3	30	0.342±0.177	0.340±0.144	0.310±0.138
Blazars	6	37	0.321±0.185	0.269±0.160	0.286±0.148
Seyferts	40	64	0.124±0.098	0.095±0.061	0.104±0.076

clude that among the sample of sources studied here, only some sources do show spectral variations. The hard X-ray band in Mrk 421 and PKS 2155−304 is primarily dominated by the non-thermal continuum (not necessarily true for the Seyfert galaxies NGC 5548 and NGC 1365), while in the soft X-ray band there can be contribution from different processes such as power law continuum, soft excess, neutral absorption and absorption features from warm absorbers. Thus, the harder when brighter trend seen in Mrk 421 and PKS 2155−304 is most likely due to changes in the power law component in the relativistic jets of these sources.

4 DISCUSSION

X-ray flux variations in AGN can be described by a wide variety of physical processes. In the radio-quiet category of objects hard X-rays can be produced by the Comptonization of soft disk photons in the hot plasma above the accretion disk (Haardt & Maraschi 1993), whereas, in the radio-loud category of AGN, hard X-rays are dominated by inverse Compton scattering of synchrotron photons by relativistic electrons in the jet via Synchrotron Self Compton process and synchrotron radiation. Given the various methods of the production of hard X-rays in AGN, there can be different causes for X-ray flux variations. In this section we discuss the results of our variability analysis, the potential causes of such variations, the nature of X-ray variations as well as their relation to various physical properties of the sources.

4.1 Flux variability

From the results of our variability analysis on a large sample of AGN belonging to different categories, we find that a major fraction of 65% of the sources in our sample show flux variability. Radio-loud objects (blazars) show large amplitude flux variations relative to their radio-quiet counterparts (Seyfert galaxies) in all the three bands, namely soft, hard and total bands. Such large amplitude flux variations are expected if the X-ray emission in radio-loud sources are dominated by radiative processes in their relativistic jets.

A total of 8 NLSy1 galaxies are in our sample. They are a separate class of AGN with soft X-ray excess (Boller et al. 1996) showing fast large amplitude X-ray flux variations (Pounds et al. 1995; Leighly 1999) and having FWHM of the Hβ line less than 2000 km s^{-1} (Osterbrock & Pogge 1985). Some of the peculiar properties of these sources have been attributed to them having higher accretions rates compared to the conventional broad line Seyfert galaxies (Peterson et al. 2000). Considering all the NLSy1 galaxies studied here as a whole, from statistical tests, no difference is found in the variability behaviour between soft and hard bands. However, three sources, namely 1H 0323+342, MCG+04−22−042 and PDS 456 show high $F_{\rm var}$ values in the hard band relative to the soft band. MCG+04−22−042, 1H 0323+342 and PDS 456 are detected at 1.4 GHz with flux densities of 10 mJy, 614 mJy and 22 mJy respectively (Condon et al. 1998). As the above three NLSy1 galaxies are detected in the radio band and as they also show more amplitude of variability in the hard band relative to the soft X-ray band, it is likely that these three sources have a significant hard X-ray contribution from relativistic jets. Of them, 1H 0323+342 is a gamma-ray emitting NLSy 1 galaxy (Abdo et al. 2009), suggesting the presence of a relativistic jet in it similar to blazars. Removing these three sources, from the list of NLSy1 galaxies and classifying the remaining sources as radio-quiet NLSy1 galaxies, we find from U test, that in radio-quiet NLSy1 galaxies variations in soft band is more than the variations in hard band. However, KS test report of no difference in $F_{\rm var}$ values between hard and soft bands. In the soft X-ray band our statistical tests indicate that radio-quiet NLSy1 galaxies are more variable than Seyfert 1 galaxies with broad optical emission lines similar to that reported by Leighly (1999). However, from both U and KS test it is evident that there is no difference in the $F_{\rm var}$ statistics in the hard X-ray band between radio-quiet NLSy1 galaxies and their broad line counterparts. This increased $F_{\rm var}$ in the soft band in radio-quiet NLSy1 galaxies might be due to them having lower BH masses than broad line Seyfert galaxies in accordance to the negative correlation between $F_{\rm var}$ and BH mass (see section 4.3). However, recently from spectro-polarimetric observations of one NLSy1 galaxy PKS 2004−447, Baldi et al. (2016) suggested that the now existing notion of NLSy1 galaxies having low BH masses need not be true and NLSy1 galaxies too have BH masses similar to blazars. If it is indeed the case, then the larger $F_{\rm var}$ seen in NLSy1 galaxies compared to their broad line counterparts might be because of them having X-ray flux variations caused by physical processes other than Seyfert 1 galaxies. In radio-quiet objects, no statistically significant differences in flux variations between soft and hard bands is found both in Seyfert 1 and Seyfert 2 galaxies. Also, we find both Seyfert 1 and Seyfert 2 galaxies showing similar $F_{\rm var}$ characteristics in all the three bands, namely, soft, hard and the full energy bands. Though these results pertain to variations on short time scales, from long term variability studies in the hard X-ray band, Seyfert 2 galaxies are found to be marginally more variable compared to Seyfert 1 galaxies (Beckmann et al. 2007; Soldi et al. 2014).

4.2 Spectral variability

To have an idea of the spectral variations of the sources relative to their brightness, correlation between HR and total flux has been studied. The HR is computed from light curves that cover a wide energy range. Therefore the disadvantage in using HR to characterize spectral variations is that they

Table 8. Results of statistical tests to compare the $F_{\rm var}$ properties of different classes of AGN

Parameters	Mann-Whitney U test				Kolmogorov-Smirnov test			
	$U_{\rm obs}$	$U_{\rm crit}$	Null hypothesis	P	D	$D_{\rm crit}$	Null hypothesis	P
Sy1 & Sy2 (soft band)	471.5	358.7	No	0.66	0.1508	0.3427	No	0.836
Sy1 & Sy2 (hard band)	492.5	358.7	No	0.88	0.1587	0.3427	No	0.787
Sy1 & Sy2 (full band)	446.0	358.7	No	0.43	0.2024	0.3427	No	0.491
BL & FSRQ (soft band)	81	54	No	0.36				
BL & FSRQ (hard band)	67	54	No	0.15				
BL & FSRQ (full band)	76	54	No	0.27				
Sy & blazars (soft band)	711	905	Yes	0.0009	0.3691	0.280872	Yes	0.002
Sy & blazars (hard band)	508	905	Yes	0.0001	0.4569	0.280872	Yes	0.000
Sy & blazars (full band)	536.5	905	Yes	0.0001	0.4573	0.280872	Yes	0.000
NLSy1 (hard v/s soft)*	59	55	No	0.0767	0.4286	0.514032	No	0.111
NLSy1 (hard v/s soft)†	33	37.6	Yes	0.0264	0.5000	0.555218	No	0.026
FSRQ (hard v/s soft)	20	8	No	0.6101				
BL (hard v/s soft)	335	316	No	0.0910	0.2667	0.351151	No	0.200
Sy1 (hard v/s soft)	387	271.8	No	0.9442	0.1071	0.363475	No	0.995
Sy2 (hard v/s soft)		473.5		0.5157	0.1111	0.320555	No	0.971
NLSy1 & BLSy1 (soft)	102	122.0	Yes	0.0128	0.5714	0.445165	Yes	0.002
NLSy1 & BLSy1 (hard)	145	122.0	No	0.177	0.3214	0.445165	No	0.237
NLSy1 & blazars (soft)	220	165.6	No	0.4237	0.2896	0.4267	No	0.306
NLSy1 & blazars (hard)	139	165.6	Yes	0.0117	0.4054	0.4267	No	0.051

*Considering all NlSy1 galaxies that include radio-quiet and radio-loud sources.
†Considering only radio-quiet NlSy1 galaxies, that include NGC 4051,
IGR J14552−5113, MCG +05−40−026 and IGR J21277+5656.

Table 9. The shortest flux doubling/halving time in minutes and its significance.

Name	Type	OBSID	τ (3−10 keV) (min.)	Sig.	τ (10−79 keV) (min.)	Sig.
3C 120	Sy1	60001042002	17.36 ± 5.60	3.11	5.25 ± 2.01	3.33
MCG +07−41−003	Sy2	60001083002	16.82 ± 5.49	3.07	9.13 ± 2.63	3.56
NGC 4051	NLSy1	60001050008	6.96 ± 1.25	5.65	5.70 ± 1.48	3.91
NGC 4151	Sy1	60001111005	16.42 ± 5.78	3.08	23.53 ± 6.36	3.70
Mrk 421	BLLac	10002015001	23.40 ± 6.66	3.52	43.40 ± 13.44	3.85
		60002023006	22.32 ± 6.80	3.29	3.04 ± 1.23	3.75
		60002023022	113.64 ± 15.26	7.71	96.20 ± 26.51	3.78
		60002023025	37.08 ± 8.69	4.27	16.59 ± 4.44	3.98
		60002023027	55.84 ± 4.72	11.57	47.44 ± 8.28	5.58
		60002023031	34.13 ± 3.47	9.84	34.72 ± 9.89	3.43
		60002023033	55.96 ± 16.92	3.31	22.33 ± 6.48	3.45
		60002023035	25.11 ± 2.54	9.88	25.07 ± 5.60	4.48
PKS 2155−304	BLLac	10002010001	10.29 ± 3.21	3.19	1.65 ± 0.16	11.67
3C 273	FSRQ	10002020001	7.29 ± 3.26	4.49	5.13 ± 0.51	10.14
IC 4329A	Sy1	60001045002	22.11 ± 7.27	3.05	14.12 ± 4.19	3.38
MCG −05−23−16	Sy1	60001046002	99.58 ± 23.12	4.23	3.35 ± 1.45	3.89
MCG −06−30−15	Sy1	60001047003	10.45 ± 3.18	3.30	7.89 ± 2.53	3.15
PDS 456	NLSy1	60002032002	4.94 ± 1.45	3.27	1.99 ± 0.85	3.34
IGR J21277+5656	NLSy1	60001110002	10.36 ± 2.84	3.68	32.59 ± 8.63	3.56
		60001110005	5.78 ± 1.93	3.79	51.47 ± 17.07	3.04
NGC 1068	Sy2	60002030004	17.63 ± 8.07	3.98	5.12 ± 1.72	3.02
NGC 1365	Sy2	60002046005	10.49 ± 2.45	4.32	5.36 ± 2.17	3.14
		60002046007	8.45 ± 2.16	3.94	7.70 ± 2.83	3.04
		60002046009	10.56 ± 3.16	3.35	7.76 ± 2.39	3.28
NGC 1052	Sy2	60061027002	3.53 ± 1.45	3.10	1.86 ± 1.02	3.67
NGC 4395	Sy2	60061322002	3.08 ± 0.44	7.33	4.35 ± 1.08	4.13

Table 10. Results of correlation analysis. Here, P and R are the probability of no correlation and the correlation coefficient respectively.

Name	OBS ID	Slope	Intercept	$\chi^2_{\rm red}$	P	R
Mrk 421	10002016001	0.005 ± 0.000	0.081 ± 0.003	0.900	$< 10^{-5}$	0.793
	60002023022	0.003 ± 0.000	0.062 ± 0.006	3.030	$< 10^{-5}$	0.802
	60002023025	0.001 ± 0.000	0.133 ± 0.000	6.954	$< 10^{-5}$	0.524
	60002023027	0.000 ± 0.000	0.119 ± 0.000	1.984	$< 10^{-5}$	0.709
	60002023031	0.000 ± 0.000	0.176 ± 0.000	2.924	$< 10^{-5}$	0.876
	60002023035	0.001 ± 0.000	0.169 ± 0.000	3.562	$< 10^{-5}$	0.646
PKS 2155−304	10002010001	0.103 ± 0.024	0.006 ± 0.029	1.995	$< 10^{-5}$	0.748
3C 273	00015012001	0.085 ± 0.034	−0.186 ± 0.262	1.193	0.010	0.735
	00015016001	0.049 ± 0.032	0.168 ± 0.187	0.984	0.029	0.658
	00015017001	−0.085 ± 0.028	1.038 ± 0.208	1.809	0.015	−0.678
NGC 5548	60002044005	−0.192 ± 0.027	1.060 ± 0.077	1.301	$< 10^{-5}$	−0.537
NGC 1365	60002046007	−0.093 ± 0.007	0.679 ± 0.018	1.890	$< 10^{-5}$	−0.718

do not identify spectral components that are responsible for the observed variations measured over a band, however, they are the simplest one to study spectral variations in a model independent way. The majority of sources in our sample do not show any correlation between HR and flux variations. However, some sources do show correlations between flux and spectral variations. In the radio-loud category, objects such as Mrk 421, PKS 2155−304 and 3C 273 (most of the time), showed a spectral hardening with increasing brightness level, i.e, a hardening when brightening trend is noticed. Among the three radio-loud sources that showed a harder when brighter trend, two sources Mrk 421 and PKS 2155−304 belong to the HSP type, where the harder when brighter trend is often seen (Giommi et al. 1990; Pian et al. 1998; Baloković et al. 2016). In the FSRQ 3C 273 (most of the FSRQs are LSP blazars), we find both harder when brighter and softer when brighter trend. We do not as yet have an unambiguous knowledge of the physical parameters that cause spectral variations. However, the harder when brighter trend seen in the three sources studied here, namely, Mrk 421, PKS 2155−304 and 3C 273 might be due to the emergence of a hard X-ray tail produced in the relativistic jets in the high brightness states in these objects. Though the overall X-ray spectrum of HSP blazars is dominated by the high energy tail of synchrotron emission (contrary to LSP blazars which is dominated by IC emission) it has recently been noticed that in the HSP blazar Mrk 421, during in its low brightness state, excess emission is noticed above 20 keV which is attributed to the emergence of the IC emission (Kataoka & Stawarz 2016). This clearly indicates that phenomena of flux and spectral variability in Mrk 421 and other blazars is complex. To identify the nature of the hard X-ray emission in our sample of radio-loud *vis-a-vis* radio-quiet sources, we generate the NuSTATR hard X-ray spectra and fit them with a simple power law model. The results of this spectral fitting for a BL Lac Mrk 421 and a Seyfert galaxy PKS 1409−651 is shown in Figure 8. From the figure it is clear that the hard X-ray emission in Mrk 421 (and other blazars) is likely dominated either by jet synchrotron or inverse Compton processes or a combination of both assuming a leptonic jet model. For Seyfert galaxies, power law model is not a good fit to the spectra, thus indicating the hard X-ray emission as due to thermal Comptonization processes. The hardening when brightening trend noticed here in the radio-loud objects Mrk 421, PKS 2155−304 and 3C 273 has been reported earlier (Malizia et al. 2000; Gliozzi et al. 2007, 2008). For two Seyfert galaxies, namely NGC 5548 and NGC 3516 a softening when brightening trend is noticed. Such softening when brightening trend is known for other Seyferts at low energies below 1 keV (Sobolewska & Papadakis 2009) as well as at energies above 2 keV (Soldi et al. 2014).

4.3 $F_{\rm var}$ v/s black hole mass

We show in Figure 7 the relation between $F_{\rm var}$ in the 3−79 keV energy range and black hole (BH) mass. The BH masses are collected from the online BH mass data base at the Georgia State University [3], which is a compilation of BH masses determined from spectroscopic monitoring observations (Bentz & Katz 2015). Of the 81 objects in our sample, BH masses are available for only 50 objects. Among those 50 objects, only 37 objects are found to be variable and they are thus used to study the correlation if any between $F_{\rm var}$ and BH mass. Figure 7 indicates that there is an anti correlation between $F_{\rm var}$ and BH mass. Both Spearmann rank correlation and Kendalls τ tests on the data indicate that the anti correlation is significant with > 99.9 percent. Using a simple linear least squares fit to the data by including the error in $F_{\rm var}$ we find

$$F_{var} = -(0.047 \pm 0.009) \times \log M_{BH} + (0.457 \pm 0.072) \quad (8)$$

Therefore, there is in general a trend for high mass objects to be less variable though there is a large scatter in the $F_{\rm var}$ v/s M_{BH} diagram. Studies of X-ray variations in the soft X-ray band on a large number of sources do show a negative correlation between $F_{\rm var}$ and BH mass similar to the one observed here (Papadakis & McHardy 1995; O'Neill et al. 2005; Ponti et al. 2012).

4.4 $F_{\rm var}$ v/s 3−10 keV luminosity

The relation between $F_{\rm var}$ and the luminosity of the source in the energy range 3−10 keV is shown in Figure 7. To determine the flux, we have fitted power law to the observed spectra for all the sources with fixed galactic column density $n_H = 1.63 \times 10^{20} cm^{-2}$. This was then used to calculate the

[3] http://www.astro.gsu.edu/AGNmass/

luminosity in the 3 − 10 keV range. From the figure there is a hint that low luminosity objects are more variable than their high luminosity counterparts.

4.5 Short time scale variability

Short time scales of flux variations in AGN taken as the flux doubling/halving time scale in this work are more often seen at high energies in the γ-ray band, for example, 4 min in PKS 2155−304 (Aharonian et al. 2007) and < 15 min in Mrk 421 (Gaidos et al. 1996) and 14 min in Mrk 421 in the NuSTAR band (Paliya et al. 2015). A recent systematic search for flux doubling/halving time scale less than 15 minutes in the soft X-ray (0.2−10 keV) band, from *Swift*/XRT observation of blazars by Pryal et al. (2015) has yielded a negative result. Observations of short time scale flux variations in the high energy band of the electromagnetic spectrum is very important, as this can set an upper limit on the size of the emitting region (R_s) via the relation $R_s < \delta c \tau_{var}/(1+z)$ and consequently, can help in constraining the emission processes. Here, τ_{var} is the time scale of variability, z is the redshift of the source and δ is the Doppler factor. Doppler factor is defined as $\delta^{-1} = \gamma(1 - \beta\cos\theta)$, where, γ is the Lorentz factor of the jet, $\beta = v/c$ is the ratio of the jet speed to the speed of light in vacuum and θ is the viewing angle, the angle between the jet and the observers line of sight. In this work, by characterising the variability time scale by either the flux doubling/halving timescale we found the shortest flux doubling/halving time scale of 1.65 ± 0.16 min for the BL Lac object PKS 2155−304. Using this observed τ_{var} we find $R_s < 2.7 \times 10^{13}(\delta/10)$ cm. Apart from PKS 2155−304, the blazars Mrk 421 and 3C 273 have also shown flux doubling/halving time scale less than 10 minutes. Such short time scales of variations are also seen in few radio-quiet sources. In our sample, we were able to derive flux doubling/halving time scale for 16 sources, of which 13 sources have time scales less than 10 min. Thus, this is the first report of the detection of statistically significant hard X-ray flux variability in a large number of AGN with flux doubling/halving time scale less than 10 minutes. The only other report of short time scale flux doubling/halving variability in the hard X-ray band available in the literature is for the source Mrk 421 (Paliya et al. 2015). On analysis of the blazar light curves for which we were able to derive flux doubling time scales, we found that the flares are asymmetric in nature showing a quick rise and slow decay similar to that observed in PKS 2155−304 and shown in Fig. 5. This might be due to the difference between the particle acceleration and synchrotron cooling time scales.

5 SUMMARY

In this work we have examined 176 observations of AGN from *NuSTAR* to search for hard X-ray flux variations in them, characterize their variability and to see how the flux variations are related to other AGN properties. Key findings of this work are summarized below

(i) A total of 81 sources (3 FSRQs, 4 BL Lac objects, 24 Seyfert 1 galaxies, 42 Seyfert 2 galaxies and 8 NLSy1 galaxies) over 176 sets of observations are studied for hard X-ray flux variability on hour time scales. We find evidence of X-ray flux variations in about 65% of the sources in our sample.

(ii) NLSy1 galaxies are found to show the highest DC of variability of about 87% followed by BL Lac objects that show a DC of 82%. Both Seyfert 1 and 2 galaxies show similar DC of about 56%. The lowest DC of variations of about 23% is shown by FSRQs.

(iii) In the 3 − 79 keV band, BL Lacs have a weighted mean $F_{\rm var}$ of 0.310 ± 0.138, while FSRQs have a weighted mean $F_{\rm var}$ of 0.093 ± 0.047. In the radio-quiet category, Seyfert 2 galaxies have a higher weighted mean $F_{\rm var}$ of 0.149 ± 0.108 relative to Seyfert 1 galaxies that have a weighted mean $F_{\rm var}$ of 0.092 ± 0.061. Both U and KS test reject the null hypothesis of differences in variability between FSRQs and BL Lac as well as Sy1 and Sy2 galaxies. In the soft X-ray band, radio-quiet NLSy1 galaxies are more variable than their broad line counterparts. Although, the BL Lacs and FSRQs examined here are more variable than the NLSy1 galaxies in the hard band, statistically in the soft bands their variations are indistinguishable.

(iv) Majority of the sources do not show any correlation between HR and count rate in the 3−79 keV energy range suggesting no spectral variability. However, a small fraction of sources show significant correlation between HR and count rate in the 3−79 keV energy range. The BL Lac objects Mrk 421 and PKS 2155−304 showed a hardening when brightening trend and the FSRQ 3C 273 showed both hardening and softening when brightening behaviour. Among the three epochs of observations, for which 3C 273 has shown variability, in two epochs a hardening when brightening trend is observed, while in one epoch a softening when brightening trend is noticed. In the radio-quiet category, two Seyfert galaxies namely, NGC 5548 and NGC 3516 showed a softening when brightening behaviour. This is opposite to that shown by the BL Lac sources Mrk 421 and PKS 2155−304.

(v) Sources hosted by massive BHs are less variable on hour time scale than their less massive counterparts. Also, $F_{\rm var}$ values show a hint for a negative correlation with luminosity of the sources in the 3−10 keV band.

(vi) We are able to estimate flux doubling/halving time scale for a total of 16 sources in our sample, of which 13 sources show flux doubling/halving time less than 10 minutes. We find the BL Lac PKS 2155−304 to show flux doubling/halving time as short as 1.65 ± 0.16 min, in the energy range 10−79 keV, the shortest ever observed in the X-ray band in any AGN.

We caution on the small number of BL Lacs, FSRQs and NLSy1 galaxies used in this work. Future observations of a large number of BL Lacs, FSRQs and NLSy1 galaxies are indeed needed to confirm the findings reported here.

ACKNOWLEDGMENTS

We thank the anonymous referee for his/her detailed comments that helped to improve the manuscript. The comments by Dr. Markus Bottcher on an initial version of the manuscript is thankfully acknowledged. This research has made use of data from the NuSTAR mission, a project led by the California Institute of Technology, managed by the Jet

Propulsion Laboratory and funded by the National Aeronautics and Space Administration. We thank the *NuSTAR* Operations, Software and Calibration teams for support with the execution and analysis of these observations. This research has made use of the *NuSTAR* Data Analysis Software (NuSTARDAS) jointly developed by the ASI Science Data Center (ASDC, Italy) and the California Institute of Technology(USA).

REFERENCES

Abdo A. A., et al., 2009, ApJ, 707, L142
Abdo A. A., et al., 2010, ApJ, 716, 30
Abeysekara A. U., et al., 2016, preprint, (arXiv:1611.04626)
Aharonian F., et al., 2007, ApJ, 664, L71
Aleksić J., et al., 2015, A&A, 578, A22
Antonucci R., 1993, ARA&A, 31, 473
Baldi R. D., Capetti A., Robinson A., Laor A., Behar E., 2016, MNRAS, 458, L69
Baloković M., et al., 2016, ApJ, 819, 156
Barthelmy S. D., et al., 2005, Space Sci. Rev., 120, 143
Beckmann V., Shrader C. R., 2012, Active Galactic Nuclei
Beckmann V., Barthelmy S. D., Courvoisier T. J.-L., Gehrels N., Soldi S., Tueller J., Wendt G., 2007, A&A, 475, 827
Bentz M. C., Katz S., 2015, PASP, 127, 67
Błażejowski M., Sikora M., Moderski R., Madejski G. M., 2000, ApJ, 545, 107
Boettcher M., Mause H., Schlickeiser R., 1997, A&A, 324, 395
Boller T., Brandt W. N., Fink H., 1996, A&A, 305, 53
Brinkmann W., Papadakis I. E., den Herder J. W. A., Haberl F., 2003, A&A, 402, 929
Caballero-Garcia M. D., Papadakis I. E., Nicastro F., Ajello M., 2012, A&A, 537, A87
Cirasuolo M., Celotti A., Magliocchetti M., Danese L., 2003, MNRAS, 346, 447
Condon J. J., Cotton W. D., Greisen E. W., Yin Q. F., Perley R. A., Taylor G. B., Broderick J. J., 1998, AJ, 115, 1693
Connolly S. D., McHardy I. M., Skipper C. J., Emmanoulopoulos D., 2016, MNRAS, 459, 3963
Dermer C. D., Schlickeiser R., 1993, ApJ, 416, 458
Edelson R., Turner T. J., Pounds K., Vaughan S., Markowitz A., Marshall H., Dobbie P., Warwick R., 2002, ApJ, 568, 610
Falcone A. D., Cui W., Finley J. P., 2004, ApJ, 601, 165
Fiore F., Laor A., Elvis M., Nicastro F., Giallongo E., 1998, ApJ, 503, 607
Foschini L., Ghisellini G., Tavecchio F., Bonnoli G., Stamerra A., 2011, A&A, 530, A77
Fossati G., et al., 2008, ApJ, 677, 906
Gaidos J. A., et al., 1996, Nature, 383, 319
Gehrels N., et al., 2004, ApJ, 611, 1005
Ghisellini G., Madau P., 1996, MNRAS, 280, 67
Ghisellini G., Haardt F., Matt G., 1994, MNRAS, 267, 743
Giommi P., Barr P., Pollock A. M. T., Garilli B., Maccagni D., 1990, ApJ, 356, 432
Gliozzi M., Brinkmann W., Räth C., Papadakis I. E., Negoro H., Scheingraber H., 2002, A&A, 391, 875
Gliozzi M., Papadakis I. E., Brinkmann W. P., 2007, ApJ, 656, 691
Gliozzi M., Papadakis I. E., Sambruna R. M., 2008, ApJ, 678, 78
Gupta A. C., Kalita N., Gaur H., Duorah K., 2016, MNRAS, 462, 1508
Haardt F., Maraschi L., 1993, ApJ, 413, 507
Haardt F., Maraschi L., Ghisellini G., 1997, ApJ, 476, 620
Harrison F. A., et al., 2013, ApJ, 770, 103
Heidt J., 1996, in Miller H. R., Webb J. R., Noble J. C., eds, Astronomical Society of the Pacific Conference Series Vol. 110, Blazar Continuum Variability. p. 64
Ivezić Ž., et al., 2002, AJ, 124, 2364
Kataoka J., Stawarz Ł., 2016, ApJ, 827, 55
Kelly B. C., Bechtold J., Siemiginowska A., 2009, ApJ, 698, 895
Konigl A., 1981, ApJ, 243, 700
Leighly K. M., 1999, ApJS, 125, 317
MacLeod C. L., et al., 2010, ApJ, 721, 1014
Malizia A., et al., 2000, MNRAS, 312, 123
Maraschi L., et al., 1999, ApJ, 526, L81
Markowitz A., Edelson R., Vaughan S., 2003, ApJ, 598, 935
McHardy I., 2010, in Belloni T., ed., Lecture Notes in Physics, Berlin Springer Verlag Vol. 794, Lecture Notes in Physics, Berlin Springer Verlag. p. 203 (arXiv:0909.2579), doi:10.1007/978-3-540-76937-8_8
McHardy I., Uttley P., Taylor R., Papadakis I., 2006, in Gaskell C. M., McHardy I. M., Peterson B. M., Sergeev S. G., eds, Astronomical Society of the Pacific Conference Series Vol. 360, Astronomical Society of the Pacific Conference Series. p. 85
Nandra K., George I. M., Mushotzky R. F., Turner T. J., Yaqoob T., 1997, ApJ, 476, 70
O'Neill P. M., Nandra K., Papadakis I. E., Turner T. J., 2005, MNRAS, 358, 1405
Osterbrock D. E., Pogge R. W., 1985, ApJ, 297, 166
Padovani P., Giommi P., 1995, ApJ, 444, 567
Paliya V. S., Böttcher M., Diltz C., Stalin C. S., Sahayanathan S., Ravikumar C. D., 2015, ApJ, 811, 143
Pancoast A., Brewer B. J., Treu T., 2014, MNRAS, 445, 3055
Papadakis I. E., McHardy I. M., 1995, MNRAS, 273, 923
Peterson B. M., et al., 2000, ApJ, 542, 161
Petrucci P. O., et al., 2000, ApJ, 540, 131
Petrucci P.-O., et al., 2013, A&A, 549, A73
Pian E., et al., 1998, ApJ, 492, L17
Ponti G., Papadakis I., Bianchi S., Guainazzi M., Matt G., Uttley P., Bonilla N. F., 2012, A&A, 542, A83
Pounds K. A., Done C., Osborne J. P., 1995, MNRAS, 277, L5
Press W. H., Teukolsky S. A., Vetterling W. T., Flannery B. P., 1992, Numerical recipes in C. The art of scientific computing
Pryal M., Falcone A., Stroh M., 2015, ApJ, 802, 33
Ravasio M., Tagliaferri G., Ghisellini G., Tavecchio F., Böttcher M., Sikora M., 2003, A&A, 408, 479
Ravasio M., Tagliaferri G., Ghisellini G., Tavecchio F., 2004, A&A, 424, 841
Rees M. J., 1984, ARA&A, 22, 471
Reis R. C., et al., 2012, ApJ, 745, 93
Romero G. E., Cellone S. A., Combi J. A., 1999, A&AS, 135, 477
Sembay S., Warwick R. S., Urry C. M., Sokoloski J., George I. M., Makino F., Ohashi T., Tashiro M., 1993, ApJ, 404, 112
Sikora M., Begelman M. C., Rees M. J., 1994, ApJ, 421, 153
Sobolewska M. A., Papadakis I. E., 2009, MNRAS, 399, 1597
Soldi S., et al., 2008, A&A, 486, 411
Soldi S., et al., 2014, A&A, 563, A57
Tagliaferri G., et al., 2000, A&A, 354, 431
Takahashi T., et al., 1996, ApJ, 470, L89
Tanihata C., et al., 2000, ApJ, 543, 124
Tanihata C., Takahashi T., Kataoka J., Madejski G. M., 2003, ApJ, 584, 153
Turner T. J., Miller L., 2009, A&ARv, 17, 47
Turner T. J., George I. M., Nandra K., Turcan D., 1999, ApJ, 524, 667
Ulrich M.-H., Maraschi L., Urry C. M., 1997, ARA&A, 35, 445
Urry C. M., Padovani P., 1995, PASP, 107, 803
Uttley P., McHardy I. M., Papadakis I. E., 2002, MNRAS, 332, 231
Vaughan S., Edelson R., Warwick R. S., Uttley P., 2003, MNRAS, 345, 1271
Véron-Cetty M.-P., Véron P., 2010, A&A, 518, A10

Wagner S. J., Witzel A., 1995, ARA&A, 33, 163
Wierzcholska A., Wagner S. J., 2016, MNRAS, 458, 56
Zhang Y. H., et al., 2002, ApJ, 572, 762
Zhang Y. H., Treves A., Celotti A., Qin Y. P., Bai J. M., 2005, ApJ, 629, 686
Zhang Y. H., Treves A., Maraschi L., Bai J. M., Liu F. K., 2006, ApJ, 637, 699
Zu Y., Kochanek C. S., Peterson B. M., 2011, ApJ, 735, 80
Zu Y., Kochanek C. S., Kozłowski S., Udalski A., 2013, ApJ, 765, 106